

The Anelastic Attenuation of Surface Waves Beneath Southwestern Arabia and the Southern Red Sea

T.A. Mokhtar

*Department of Geophysics, Faculty of Earth Sciences,
King Abdulaziz University, P.O. Box 80206, Jeddah 21589,
Kingdom of Saudi Arabia, Email: tmokhtar@kau.edu.sa*

Received: 23/4/2005

Accepted: 30/4/2006

Abstract. The seismic attenuation coefficients of surface waves in southwestern Arabian Peninsula and the southern Red Sea were investigated using the station ratio method. Love and Rayleigh waves data recorded by two GSN stations RAYN and ATD are used to compute Love and Rayleigh waves attenuation coefficients (γ_L and γ_R), and Love and Rayleigh waves internal friction (Quality factors, Q_L and Q_R) in the region between the two GSN seismic stations RAYN and ATD. RAYN lies at the center of Arabia, while ATD is located on the western coast of the southern Red Sea on the Afar depression. γ_R is found to vary from a low of $4.03 \times 10^{-4} \text{ km}^{-1}$ at 27 s and a high of $22.9 \times 10^{-4} \text{ km}^{-1}$ at 44 s. γ_L , on the other hand, varies between a minimum of $-2.28 \times 10^{-4} \text{ km}^{-1}$ at 6 s and a maximum of $10.81 \times 10^{-4} \text{ km}^{-1}$ at 23 s. The average quality factors Q_R and Q_L for the upper crust are estimated to be 100 and 160, respectively. Surface wave attenuation below the upper crust is extremely high. The high attenuation of the crust and upper mantle may be explained in the frame work of the ongoing tectonic process of the Red Sea and the Afar depression. High temperature associated with partial melting beneath the crust can result in increasing the attenuation which is observed at long periods, while at short periods (less than 27 s), the level of attenuation is less. However, the attenuation is remarkably high. The results of this confirm previous indications that the Arabian plate, unlike other stable regions, has unusually higher attenuation characteristics for seismic waves in the crust and upper mantle comparable to many tectonically active regions of the world.

Introduction

Seismic hazard studies require that the seismic wave attenuation of the region of interest be well determined. The past few decades have seen a remarkable increase in the quality of surface wave attenuation studies for various regions of the earth and in the determination of the effect of seismic wave internal friction (quality factor) Q (e.g. Mitchell, 1980).

Research has shown that much of the variability in estimates of peak ground motion values is due to uncertainties inherent in ground motion attenuation models (e.g. Bender, 1984, McGuire and Shedlock, 1981).

The anelastic attenuation of seismic waves of the Arabian Peninsula, however, has not been investigated very well. The amount of data about the values of attenuation coefficients and the quality factors in the region, which was provided by few studies, was too little to provide sound and undisputable results (e.g. Mokhtar (1987), Mokhtar *et al.*, (1988), Seber (1990), Seber and Mitchell (1992), Ghalib (1992), and Mokhtar (1995)). Mokhtar (1987) investigated Q_B (shear wave quality factor) for the top 1.0 km thickness of the crust of the Arabian shield using very short period Rayleigh waves signals (1.0 to 20.0 Hz) which were recorded in a deep seismic refraction profile survey which was carried out across the shield (Fig. 1, Healy *et al.*, 1982). Mokhtar (1987) analyzed the decay of Rayleigh wave amplitudes with distance at different frequencies and found that the Rayleigh wave attenuation coefficient (γ_R) decreased from 0.3 km^{-1} at 0.1 s period to $0.006\text{-}0.015 \text{ km}^{-1}$ at 0.8 s period. Inversion of γ_R showed that Q_B values increased from 30 in the upper 50 m of the crust to 150 at a depth of 0.5 km. It was also found that Q_B is very sensitive to lithological changes and to the geological structures of formations as determined by the degree of faulting and lineation in the rock.

Ghalib (1992) presented the value of 0.0045 km^{-1} for the attenuation coefficient at 1.0 Hz of high frequency seismic data from the Arabian plate. He applied the extended coda quality factor technique to short period L_g coda waves. This technique was based on least squares principles and provided a deterministic procedure for estimating coda Q and its frequency dependence simultaneously. It was found by Ghalib (1992) that the Arabian plate has surprisingly low Q values. This was attributed to the relatively young age of the Arabian shield and its intensive metamorphism and deformation.

Likewise, Seber and Mitchell (1992) studied the attenuation of surface waves across the Arabian Peninsula. They computed slopes of observed and predicted amplitude spectra of the fundamental mode Rayleigh and Love waves to determine Q model for the upper crust. They concluded that Q values of the Arabian plate vary from 60 along the margin of the Red Sea to 100-150 in the central

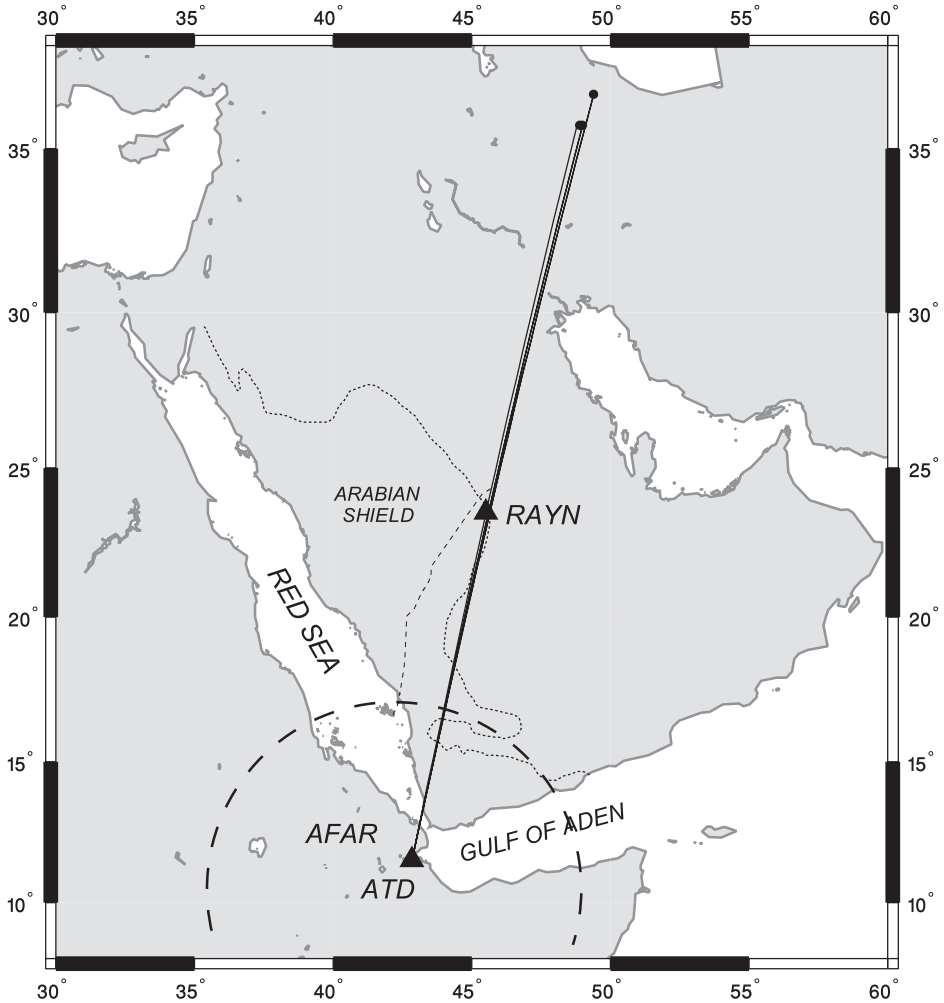


Fig. 1. The locations of the earthquakes used in this study and the two seismic stations RAYN and ATD. The solid lines represent the great circle path from the events to the stations. Dotted line marks the boundary of the Arabian shield. The dark dashed circle is the boundary of the Afar plume head as proposed by Knox *et al.* (1998), and the light dashed line is the location of the deep seismic refraction line (Healy *et al.*, 1982).

part of Arabia, to 60-80 in the eastern folded region. Compared to other shields and stable regions, these values are considered to be unusually low.

More recently, Mokhtar (1995) used a general Q model for the Arabian platform to compute synthetic seismograms in an attempt to test shear wave velocity models of the platform, derived by Mokhtar and Al-Saeed (1994). The quality factor model consisted of an upper crust with Q_{α} (compressional wave quality

factor) = 160 and $Q_B = 80$ and a lower crust with $Q_\alpha = 300$ and $Q_B = 150$. The wave forms of all components were successfully modeled using such Q values, however, due to the lack of magnification information of RYD (Riyadh) station, he was unable to obtain reliable Q estimates from the data used.

Evidence of major increase of Lg attenuation relative to Pg across the boundary between the Arabian and the Eurasian plates was observed by Sandvol *et al.* (2001). Lg propagation within the Arabian plate was found to be generally efficient compared to the regions of the Anatolian and Iranian plateaus.

Thenhaus, *et al.* (1989) presented estimates of seismic horizontal ground acceleration and velocity for western Saudi Arabia. Due to the lack of strong ground motion data for the Arabian Peninsula, their results were based on two assumed models, a preferred low Q attenuation model, and a conservative high Q attenuation model.

This study presents computed values of γ_R , γ_L , Q_R , and Q_L for the crust and upper mantle beneath the region close to the southern edge of the Arabian shield and beneath the southern Red Sea region by using observed data from two GSN seismic network stations RAYN and ATD.

Determination of Surface Waves Attenuation

The complex spectra of seismic surface waves at a seismic station can be represented by (Báth, 1982)

$$|A(\omega, r)| = |S(\omega)| |B(\theta)| |C(\omega, r)| |G(r)| |I(\omega)| e^{-\gamma r} \quad (1)$$

Where $S(\omega)$ is the source spectrum, corresponding to source time function, is the source space function, $B(\theta)$ where θ stands for direction from the source to the station (directivity function), $C(\omega, r)$ is the propagation path effect on surface waves amplitude, $G(r)$ is the geometrical spreading, $I(\omega)$ is the instrumental response, γ is the attenuation coefficient, and r is the distance between the epicenter and the station. Let us consider the surface wave spectrum observed at two stations lying at distances r_1 , and r_2 along the same azimuth from an earthquake and on the great circle path, and ω is the angular frequency. If the two stations have similar instrumentations or if the instrument effect of each station was removed from the spectrum, then we can take the ratios of the corrected spectral amplitudes of the events at these two stations to obtain the average attenuation coefficient below the region between them. By taking the spectral amplitude ratio at the two stations, all the parameters related to the seismic source will be cancelled out.

Ben-Menahem (1965) showed that the attenuation coefficients of surface waves can be computed from the amplitude of the events at two stations by means of the relation

$$\gamma(\omega) = \ln[A(\omega, r_1) / A(\omega, r_2)] / (r_2 - r_1). \quad (2)$$

Where $A(\omega, r_1)$ and $A(\omega, r_2)$ are the corrected spectral amplitudes of the waves at the two stations having epicentral distances r_1 and r_2 (in kilometers). Q could then be derived from the attenuation coefficient $\gamma(\omega)$ and the group velocity U as:

$$Q = \omega / 2\gamma(\omega)U(\omega) \quad (3)$$

Attenuation coefficients of Rayleigh and Love waves, in the period range 1-60 seconds were computed from the two GSN stations RAYN and ATD recordings for 3 major earthquakes located in northern Iran and are lying on a great circle path with the two stations (Fig. (1)). The parameters of these events are listed in Table (1). The vertical and transverse components of the events from the two stations were used in these computations. Seismograms displaying Rayleigh and Love waves from these two stations for the events listed in Table 1 are shown in Fig. 2 and Fig. 3.

The vertical component (BHZ) and the two horizontal components (BHN and BHE) of each event were corrected for instrument response and filtered using a band-pass Butterworth filter with corner frequencies at 0.01 Hz and 1.0 Hz. Instrument response corrections were performed using the poles and zeros values provided for each station and each component. The two horizontal components were then rotated to produce radial and transverse (Love) components. The time series of each component was transformed using Fast Fourier Transform (FFT) and γ_R was computed from the vertical components while γ_L was computed from the transverse components.

For each component, the corrected spectrum was interpolated using cubic spline interpolation at a spectral interval of 1 second period. Fig. 4 displays the amplitude spectra for all 3 used events listed in Table 1. Notice the drop of the amplitude from the close station (RAYN) to the distant station (ATD). γ_R and γ_L were then computed at the interpolated periods using equation (2), while Q_R , and Q_L were determined from equation (3). The group velocities used in these calculations are those determined by Mokhtar (2004) for the southwestern path of the Arabian Peninsula which, more or less, coincide with the section of the great circle path between RAYN and ATD. Tables (2) and (3) list γ_R and γ_L for the periods 1-60 seconds, and Q_R and Q_L for the periods from 5 to 47 seconds. Figure (5) shows the variations of γ_R and γ_L as a function of period.

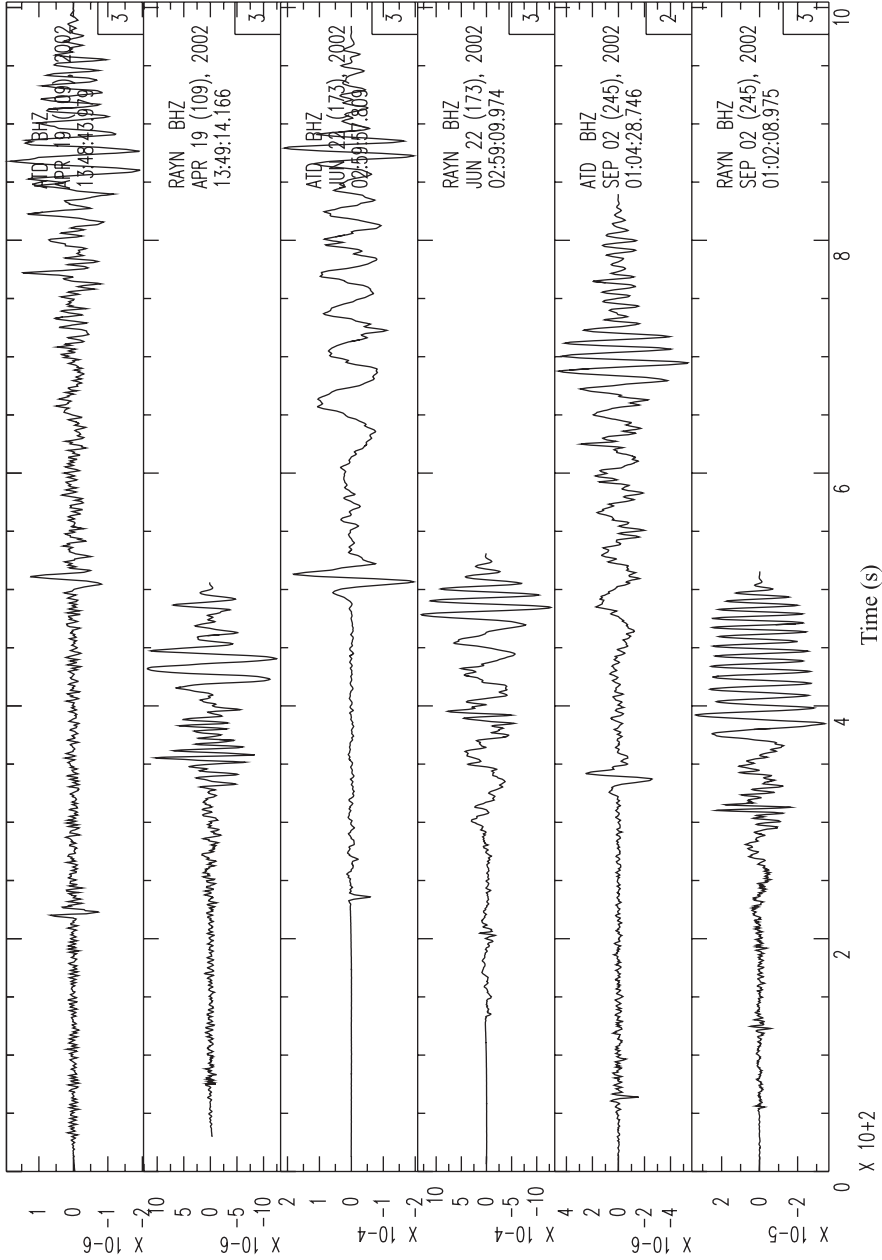


Fig. 2. The vertical component (Rayleigh waves) of the earthquakes listed in Table 1 recorded by RAYN and ATD seismic stations.

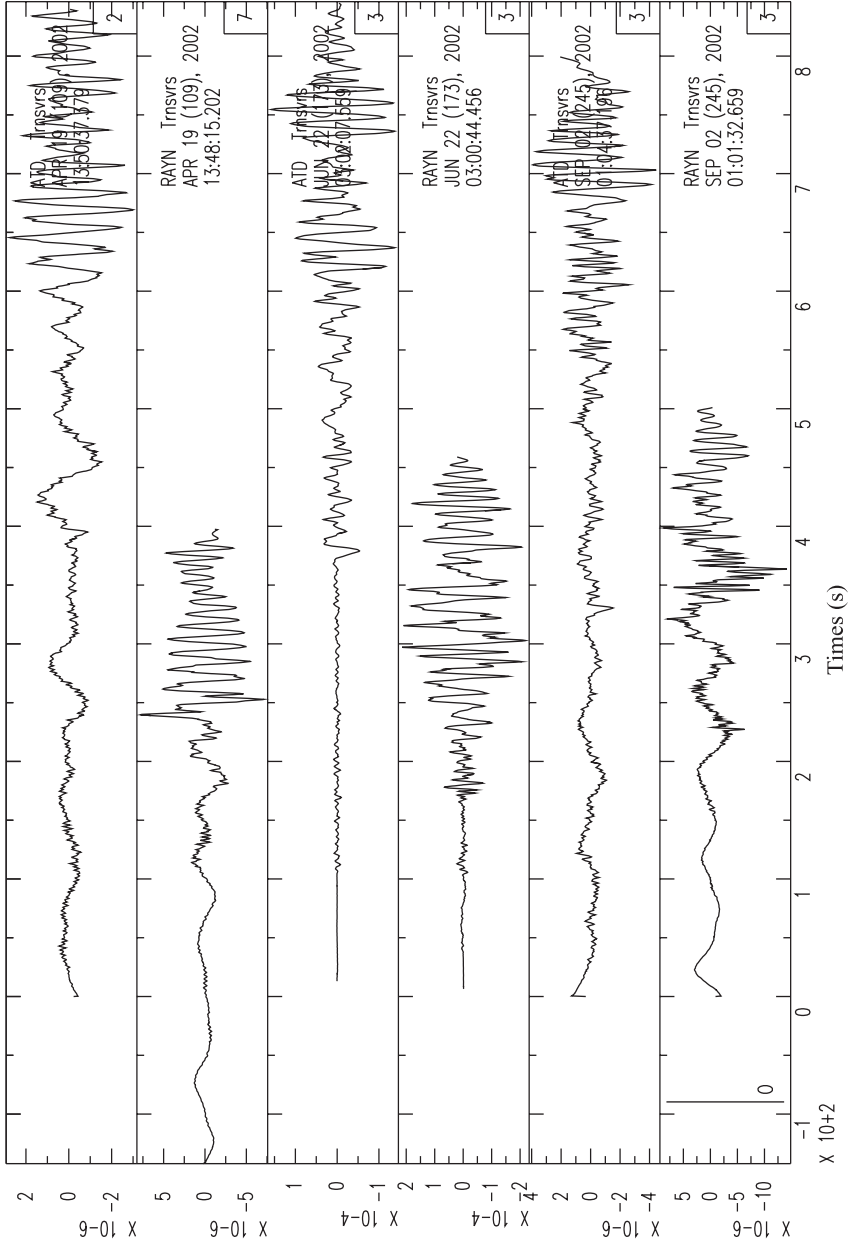


Fig. 3. The horizontal component (Love waves) of the earthquakes listed in Table 1 produced by the rotation of the E-W and the N-S horizontal components recorded by RAYN and ATD seismic stations.

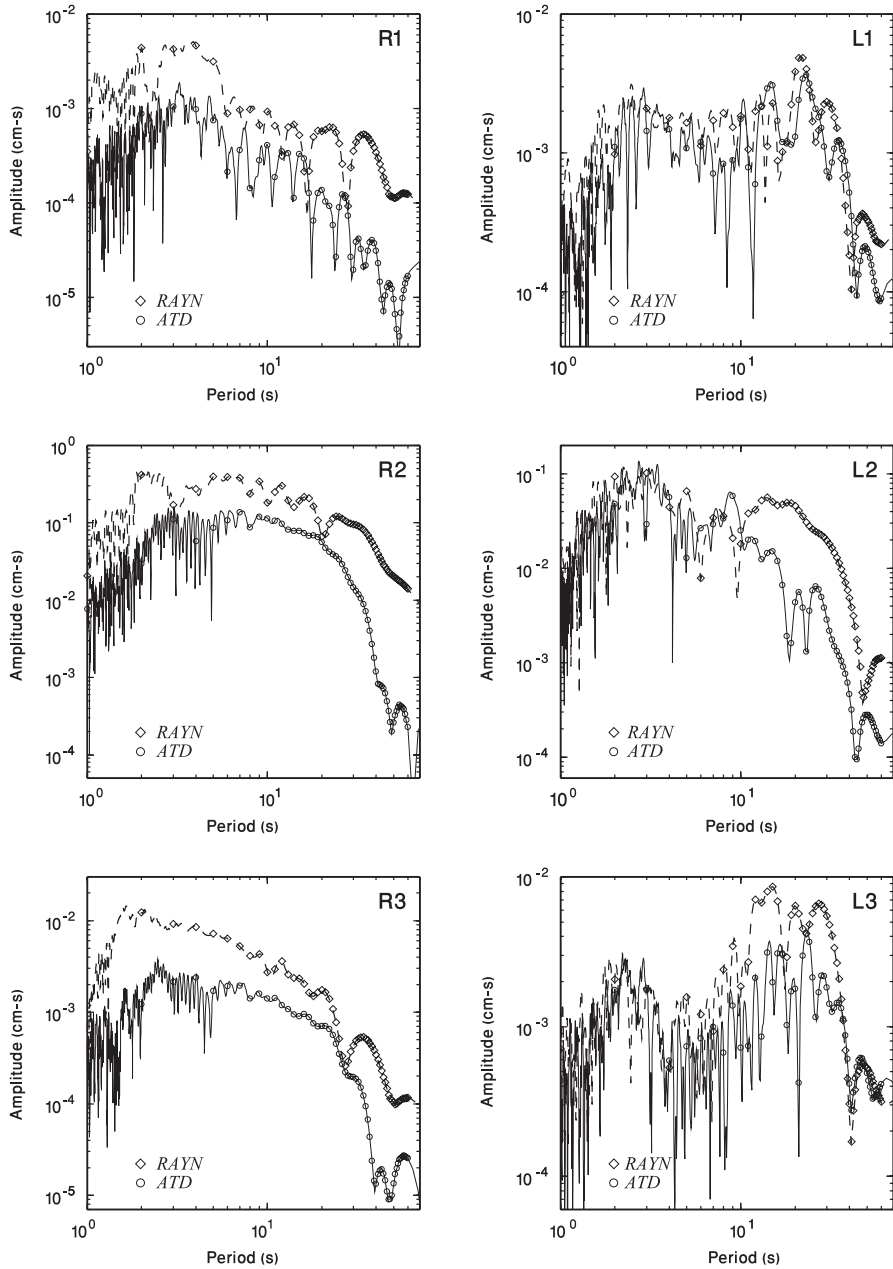


Fig. 4. The amplitude spectra obtained from the process of FFT for the six components from RAYN and ATD stations. The open diamonds and open circles represent the 1 s spectral interpolated values used in the computation of the attenuation coefficients. R is for Rayleigh and L is for Love, while the numbers represent the event number in Table 1.

Table 1. Source parameters of the earthquakes used in this study.

	Date			Origin Time			Hypocenter			Magnitude	
	Y	M	D	H	M	S	Lat°	Lon°	H (km)	Mb	Ms
1	2002	04	19	13	46	49.77	36.567	49.810	33	5.2	
2	2002	06	22	02	58	21.30	35.626	49.047	10	6.2	6.4
3	2002	09	02	01	00	03.27	35.701	48.838	10	5.1	4.7

γ_R is found to vary from $16.03 \times 10^{-4} \text{ km}^{-1}$ at 2 s to $5.48 \times 10^{-4} \text{ km}^{-1}$ at 17 s. γ_R values beyond 17 s increase to reach $11.64 \times 10^{-4} \text{ km}^{-1}$ at 24 s then it falls down again to $4.03 \times 10^{-4} \text{ km}^{-1}$ at 27 s. The value of γ_R increases again beyond 27 s and reaches about $22.90 \times 10^{-4} \text{ km}^{-1}$ at 44 s where it decreases slightly beyond this period and reaches $18.64 \times 10^{-4} \text{ km}^{-1}$ at 60 s. Q_R , which is obtained by using equation (3) above and the values of computed γ_R listed in Table 2, shows a decrease from about 240 at 5 s period to about 8 at 47 s.

On the other hand, γ_L values show higher scatters than γ_R , and oscillates in the average between a low of $-2.28 \times 10^{-4} \text{ km}^{-1}$ at 6 s and a high of $12.91 \times 10^{-4} \text{ km}^{-1}$ at 21 s. Computed Q_L decreases from a slightly high value of 376 at 5 s period to about 53 at 47 s with a maximum of 735 at 7 s and a minimum of 17 at 44 s (Table 3).

The Effect of Afar Hotspot on Surface Wave Attenuation

Several studies have indicated the presence of an upper mantle thermal anomaly situated beneath the Afar depression and south western Arabian Peninsula (e.g. Ritsema and Allen, 2003; Ritsema *et al.*, 1999; Knox *et al.*, 1998). It is widely accepted that the tectonism and geology of Afar depression is strongly affected by the presence of a mantle plume beneath it. Several evidences have been presented to support this conclusion including the presence of an upper mantle thermal anomaly associated with a low seismic shear wave velocity anomaly (Ritsema and Allen, 2003), and the temporal sequence of uplift, volcanism and rifting (Menzies *et al.*, 1992). The boundary of the Afar plume head is shown in Fig. 1 as proposed by Knox *et al.* (1998).

The presence of the mantle plume is supported also by models derived from seismic refraction profiles and short period surface waves which indicate a thin crust and an anomalous seismically slow uppermost mantle beneath Afar (Makris and Ginzburg, 1987). Knox *et al.* (1998) used phase velocities of Rayleigh wave dispersion from three paths crossing the Afro-Arabian dome to map the upper mantle S wave velocities beneath Afar and western Saudi Arabia. The uppermost mantle beneath Afar and western Saudi Arabia is char-

acterized by pronounced negative S wave velocity gradients and S wave velocities between 0.2 and 0.8 km/s, which are lower than the Preliminary Reference Earth Model (PREM) of Dziewonski and Anderson (1981) at 100 km depth. These results are consistent with a thermal plume model for Afar, having a few percent of partial melt within the mantle (Knox *et al.*, 1998).

ATD station lies on the eastern coast of the Afar depression (Fig. 1). The geology beneath the station consists of weathered basalt. As shown in Fig. 5, the attenuation coefficients of Rayleigh waves are unusually high especially for periods longer than 27 s, and reach a high of about $22.90 \times 10^{-4} \text{ km}^{-1}$ at 44 s. It remains high for long periods, but beyond 44 s it decreases to $18.64 \times 10^{-4} \text{ km}^{-1}$ at 60 s. The high attenuation values for longer periods could be explained by the presence of the low velocity anomalous thermal plume underlying the crust of the Afar depression which clearly has a strong attenuation effect on Rayleigh waves which were recorded at ATD. It is obvious, however, that a similar conclusion can not be drawn for Love waves (Fig. 5). This is due to the high noise levels on some seismograms especially in the case of events 1 and 3 (Fig. 4). However, at least one Love wave spectrum (event 2) shows similar drop in the amplitude from RAYN to ATD. The use of Love waves is important as they help provide additional Q investigations for the same path as that provided by Rayleigh waves. Unfortunately, additional data from other events along the same path and for the same regional distances are not available for the great circle path that include the two stations. However, the scope of this work is to obtain some average of the attenuation of the crust in the region of southwestern Arabia and the southern Red Sea, and the results from Rayleigh waves should be considered more reliable in this regard.

Seber and Mitchell (1992) obtained shear wave Q values in the upper crust by fitting the slope of the amplitude spectra at short periods (5-30 s). Using a model of 20 km upper crust overlying a half space for the Arabian plate, it was found that the half space Q values had no significant effect on the amplitude spectra at shorter periods, while Q values in the upper crust had a larger effect on the amplitude spectra at shorter periods, 1-30s, (Seber and Mitchell, 1992).

Taking the effect of the Afar plume on the amplitude spectrum at long periods, and assuming that the effect of the upper crust Q on the amplitude spectra is mainly at short periods, one can assume that the values of γ_R and γ_L at periods less than 27 could be taken to represent the average attenuation in the upper crust in the region between RAYN and ATD stations. Accordingly, revised calculations show that the average γ_R and γ_L for the period range 5 to 27 s are $7.97 \times 10^{-4} \text{ km}^{-1}$ and $6.14 \times 10^{-4} \text{ km}^{-1}$, respectively. Using the surface wave Q values listed in Tables 2 and 3 for periods less than 27 s, the average Q_R and Q_L are found to be 100 and 160, respectively.

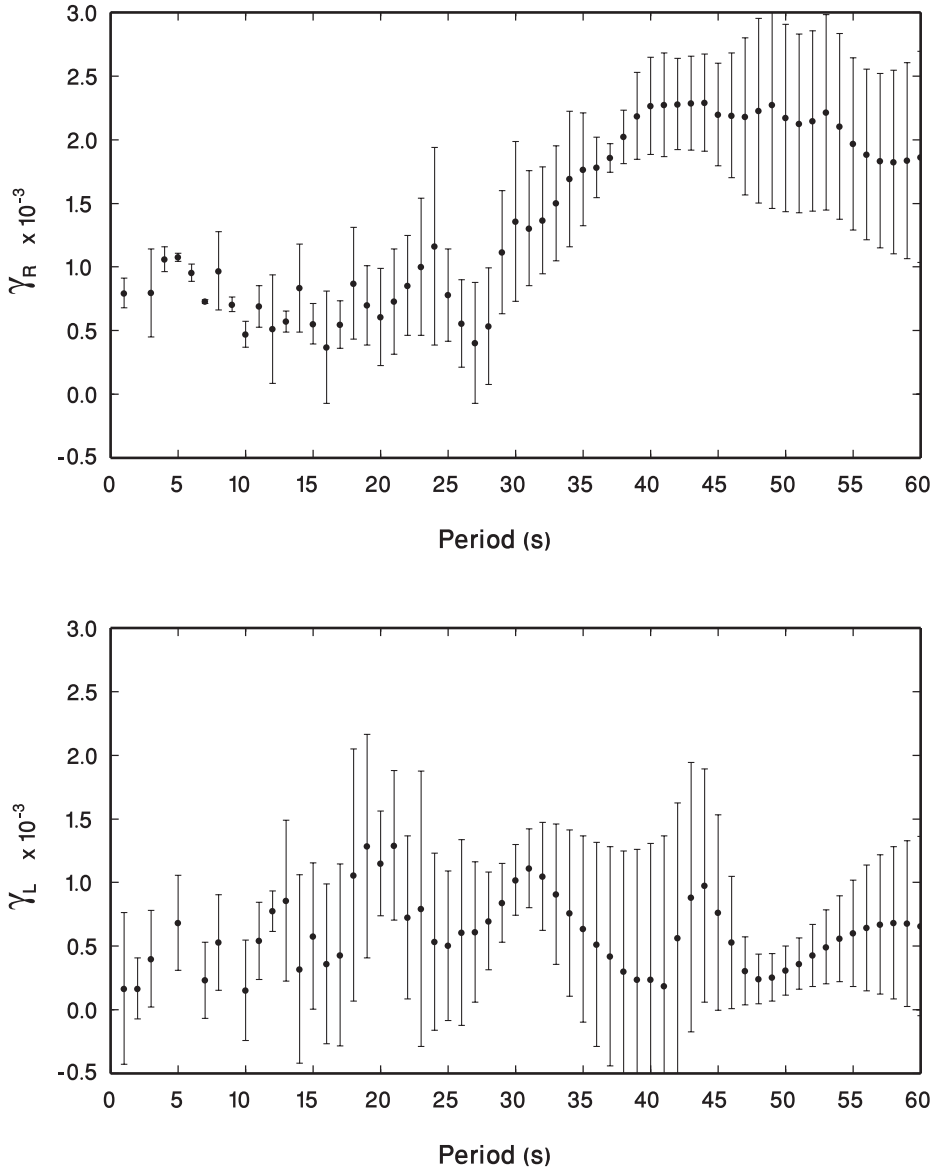


Fig. 5. The Rayleigh wave attenuation coefficient (γ_R) and Love wave attenuation coefficient (γ_L) for southwestern Arabia and the southern Red Sea region.

Table 2. Rayleigh waves attenuation coefficients for southwestern Arabia and the southern Red Sea.

Period (S)	Computed γ_R $\text{km}^{-1} \times 10^4$			Average γ_R $\text{km}^{-1} \times 10^4$	Standard deviation $\text{km}^{-1} \times 10^4$	Group velocity km / s	Q_R
	Event 1	Event 2	Event 3				
1.	9.61	7.22	7.03	7.95	1.17		
2.	11.73	19.37	16.98	16.03	3.19		
3.	10.24	3.08	10.58	7.97	3.48		
4.	11.34	11.29	9.25	10.63	0.98		
5.	10.49	11.20	10.59	10.76	0.31	2.42	241
6.	10.41	9.44	8.76	9.54	0.67	2.55	215
7.	7.11	7.48	7.27	7.29	0.15	2.63	234
8.	14.05	7.23	7.82	9.70	3.085	2.71	149
9.	6.28	7.61	7.29	7.06	0.57	2.86	173
10.	5.92	3.41	4.80	4.71	1.03	2.97	225
11.	9.18	6.20	5.37	6.92	1.64	3.03	136
12.	-0.91	8.26	8.02	8.14	4.2	3.09	104
13.	4.54	6.23	6.38	5.72	0.84	3.12	136
14.	13.15	5.18	6.71	8.35	3.45	3.13	86
15.	3.29	6.43	6.90	5.54	1.60	3.14	120
16.	-2.41	7.85	5.61	6.73	4.4	3.15	93
17.	3.83	8.10	4.50	5.48	1.88	3.17	107
18.	14.91	6.27	4.99	8.72	4.41	3.18	63
19.	11.11	3.56	6.31	6.99	3.12	3.19	74
20.	10.45	1.17	6.61	6.08	3.81	3.21	81
21.	12.80	2.88	6.18	7.29	4.12	3.23	64
22.	14.07	6.05	5.53	8.55	3.91	3.26	51
23.	17.44	7.83	4.78	10.02	5.39	3.28	42
24.	22.28	8.69	3.94	11.64	7.77	3.31	34
25.	11.35	9.23	2.83	7.81	3.63	3.34	48
26.	5.35	9.87	1.478	5.57	3.43	3.37	65
27.	0.26	10.74	1.09	4.03	4.76	3.40	85
28.	1.60	11.79	2.63	5.34	4.58	3.43	61
29.	16.04	12.87	4.56	11.15	4.84	3.5	28
30.	21.22	13.71	5.84	13.59	6.28	3.5	22

Table 2. Contd.

Period (S)	Computed γ_R $\text{km}^{-1} \times 10^4$			Average γ_R $\text{km}^{-1} \times 10^4$	Standard deviation $\text{km}^{-1} \times 10^4$	Group velocity km / s	Q_R
	Event 1	Event 2	Event 3				
31.	17.86	14.30	6.97	13.05	4.53	3.53	22
32.	18.17	14.81	8.07	13.68	4.20	3.56	20
33.	20.35	15.39	9.29	15.01	4.53	3.57	18
34.	23.76	16.19	10.80	16.92	5.32	3.58	15
35.	23.33	17.18	12.49	17.67	4.44	3.60	14
36.	20.38	18.46	14.66	17.83	2.38	3.61	14
37.	18.30	20.08	17.34	18.57	1.13	3.60	13
38.	17.30	22.19	21.18	20.22	2.11	3.60	11
39.	17.07	24.46	24.10	21.88	3.40	3.60	10
40.	17.50	26.57	23.92	22.66	3.81	3.62	10
41.	18.74	28.34	21.17	22.75	4.08	3.63	9
42.	21.13	27.80	19.51	22.81	3.58	3.64	9
43.	23.13	27.29	18.23	22.88	3.70	3.65	9
44.	23.92	26.98	17.81	22.90	3.81	3.67	9
45.	20.29	27.52	18.12	21.98	4.02	3.70	9
46.	17.81	28.81	19.10	21.91	4.91	3.72	8
47.	15.92	30.35	19.23	21.83	6.17	3.74	8
48.	15.8201	32.4243	18.5774	22.27	7.27		
49.	16.4411	34.1928	17.5676	22.73	8.12		
50.	18.1733	31.9518	14.9961	21.70	7.36		
51.	20.8008	30.1104	12.9221	21.28	7.03		
52.	23.5916	28.8972	11.9383	21.48	7.08		
53.	27.3132	27.8741	11.2797	22.16	7.69		
54.	25.3233	27.0193	10.7633	21.04	7.30		
55.	21.241	27.0529	10.7248	19.67	6.76		
56.	18.8035	27.0883	10.664	18.85	6.71		
57.	17.3103	27.1967	10.5084	18.34	6.85		
58.	16.0578	27.9907	10.7152	18.26	7.22		
59.	15.1862	28.9618	10.9254	18.36	7.70		
60.	14.6046	30.1891	11.139	18.64	8.29		

Table 3. Love waves attenuation coefficients for southwestern Arabia and the southern Red Sea.

Period (S)	Computed γ_L $\text{km}^{-1} \times 10^4$			Average γ_L $\text{km}^{-1} \times 10^4$	Standard deviation $\text{km}^{-1} \times 10^4$	Group velocity km / s	Q_L
	Event 1	Event 2	Event 3				
1.	-6.35	7.83	3.55	1.67	5.94		
2.	-0.97	4.83	1.17	1.67	2.39		
3.	2.677	9.19	0.15	4.00	3.80		
4.	1.29	-1.86	-0.86	-0.47	1.31		
5.	3.06	11.92	5.56	6.84	3.72	2.44	376
6.	-0.48	-9.05	2.69	-2.28	4.96	2.57	
7.	6.45	1.08	-0.55	2.32	2.99	2.63	735
8.	6.15	0.32	9.39	5.29	3.75	2.73	272
9.	-3.94	-7.67	6.70	-1.63	6.23	2.85	
10.	0.29	-2.54	6.89	1.54	3.95	2.94	694
11.	2.14	4.67	9.46	5.42	3.03	3.03	173
12.	8.90	5.52	8.81	7.74	1.57	3.10	109
13.	0.05	10.47	15.17	8.56	6.31	3.17	89
14.	-7.13	9.85	6.86	3.19	7.40	3.24	217
15.	-2.26	8.83	10.78	5.78	5.74	3.31	109
16.	-4.97	9.92	5.89	3.61	6.29	3.37	161
17.	-1.27	14.3	-0.16	4.31	7.12	3.41	125
18.	0.19	23.89	7.65	10.58	9.89	3.45	47
19.	4.89	25.11	8.61	12.87	8.78	3.50	36
20.	7.89	17.25	9.32	11.49	4.11	3.55	38
21.	5.06	14.53	19.15	12.91	5.86	3.57	32
22.	2.47	16.31	2.99	7.26	6.40	3.58	54
23.	0.66	23.22	-0.08	7.93	10.81	3.585	48
24.	-0.92	15.04	1.94	5.35	6.95	3.59	68
25.	-2.99	10.90	7.19	5.03	5.87	3.61	69
26.	-4.14	9.79	12.52	6.06	7.29	3.64	54
27.	-1.66	9.99	10.02	6.11	5.50	3.66	52
28.	1.87	11.07	7.99	6.98	3.82	3.68	43
29.	5.14	12.54	7.52	8.40	3.08	3.70	34
30.	8.39	14.11	8.06	10.19	2.77	3.73	27

Table 3. Contd.

Period (S)	Computed γ_L $\text{km}^{-1} \times 10^4$			Average γ_L $\text{km}^{-1} \times 10^4$	Standard deviation $\text{km}^{-1} \times 10^4$	Group velocity km / s	Q_L
	Event 1	Event 2	Event 3				
31.	8.96	15.48	8.93	11.12	3.08	3.77	24
32.	6.45	16.34	8.62	10.47	4.24	3.82	24
33.	3.78	16.69	6.74	9.07	5.52	3.88	27
34.	1.60	6.68	4.49	7.59	6.53	3.91	31
35.	-0.18	16.54	2.69	6.35	7.30	3.90	36
36.	-1.89	16.32	0.97	5.13	8.00	3.89	43
37.	-3.40	16.24	-0.24	4.20	8.61	3.95	51
38.	-5.50	16.23	-1.72	3.00	9.48	4.01	68
39.	-7.05	16.53	-2.27	2.40	10.18	4.01	83
40.	-7.72	17.18	-2.31	2.38	10.69	4.01	82
41.	-9.06	18.27	-3.61	1.86	11.81	4.01	102
42.	-1.64	20.66	-2.10	5.63	10.62	4.03	32
43.	4.39	23.46	-1.31	8.84	10.59	4.05	20
44.	8.87	21.40	-0.97	9.76	9.15	4.07	17
45.	6.68	17.48	-1.25	7.63	7.68	4.06	22
46.	5.35	11.60	-1.09	5.28	5.18	4.04	32
47.	4.52	5.320	-0.66	3.06	2.65	4.06	53
48.	3.97	3.587	-0.31	2.41	1.93		
49.	3.49	4.194	-0.03	2.55	1.85		
50.	3.49	5.22	0.51	3.08	1.94		
51.	3.60	6.14	1.15	3.63	2.03		
52.	3.90	7.43	1.47	4.27	2.44		
53.	4.32	8.76	1.72	4.94	2.90		
54.	4.79	10.06	1.92	5.59	3.36		
55.	5.33	11.41	1.28	6.01	4.16		
56.	5.96	12.71	0.64	6.44	4.93		
57.	6.43	13.56	0.16	6.72	5.47		
58.	6.94	14.08	-0.56	6.82	5.98		
59.	7.00	14.63	-1.29	6.78	6.50		
60.	6.56	15.21	-2.02	6.58	7.03		

Discussions and Conclusions

The anelastic attenuation of seismic waves in the earth is not well understood. Anelastic variations with changes in the physical state are complicated and probably can not be explained by a single model or mechanism. As a result, a variety of mechanisms have been proposed in the past and recent years in order to explain observations of anelastic seismic attenuation in different regions of the earth. The seismic wave attenuation observed in near surface rocks, which usually contain cracks, joints, and fractures, is attributed to frictional dissipation as crack surfaces in contact slide relative to one another during the passage of seismic waves (*e.g.* Walsh, 1966). Also, since most of the near surface rocks contain fluids in their pores, an alternative model for attenuation was developed that is based on the flow of pore fluid relative to the rock containing them (*e.g.* Winkler & Nur, 1982; Toksöz *et al.*, 1979). Such mechanisms, however, can not explain the observed attenuation in the deeper parts of the earth, such as the lower crust and the upper and lower mantle, where cracks are completely closed and pores no longer exist due to the compaction as a result of increased pressure at depth.

The Arabian shield, which constitutes about one third of the Arabian plate, was formed by successive accretions of newly formed crust between 1000 and 700 Ma (Shmidt *et al.*, 1979). Successively younger island arcs formed to the east as west dipping subduction zones shifted eastward. The oceanic crust that was formed originally has evolved into the new thick continental crust by a series of subsequent compressional orogenies and episodes of intrusions and volcanisms which ceased about 620 Ma (Alshanti, 1992). The higher shear wave velocity in the upper crust of the Arabian shield is attributed to the presence of the ophiolitic belts which represent the remnants of the old oceanic crust (Mokhtar and Al Saeed, 1994; Mokhtar *et al.*, 2001; Rodgers *et al.*, 1999). The Arabian shield is characterized by lateral inhomogeneities and the presence of lateral variations and deformations within the crust (Healy *et al.*, 1982). This conclusion was based on the observations of significant deviations of observed arrival times of the first P waves recorded by a deep seismic refraction profile across the shield from the predicted arrivals. Gettings (1986) identified several lateral inhomogeneities in the bulk physical properties in both the upper and lower crust of the shield, indicating bulk compositional variations and the presence of structural deformations. His conclusion was based on an integrated interpretation of seismic data from the refraction profile mentioned before and regional gravity, aeromagnetism, heat flow, and surface geology data of the Arabian shield.

Thus, by comparing the southwestern Arabian Peninsula and the southern Red Sea with other regions, it is found that the attenuation of long period surface waves at these two regions is extremely higher than at other regions. For exam-

ple, Fig. 6 shows a comparison between Q_L and Q_R obtained from this study and those obtained by Solomon (1972) for the western United States. Q_R values beneath the Arabian Peninsula are lower than those for the western United States by several orders of magnitudes especially for periods greater than 27 s. Similar conclusion can be drawn for Q_L . However the difference is less pronounced than in the case of Q_R . This increase in attenuation is believed to be due to the effect of the hot spot situated beneath the Afar region as explained before. It is likely that a large part of the upper mantle beneath southwestern Arabian Peninsula and the southern Red Sea region is partially melted resulting in a very low Q zone. This low-Q zone cannot be entirely the result of high temperature gradients, phase transformations or changes in composition (Anderson and Sammis, 1970).

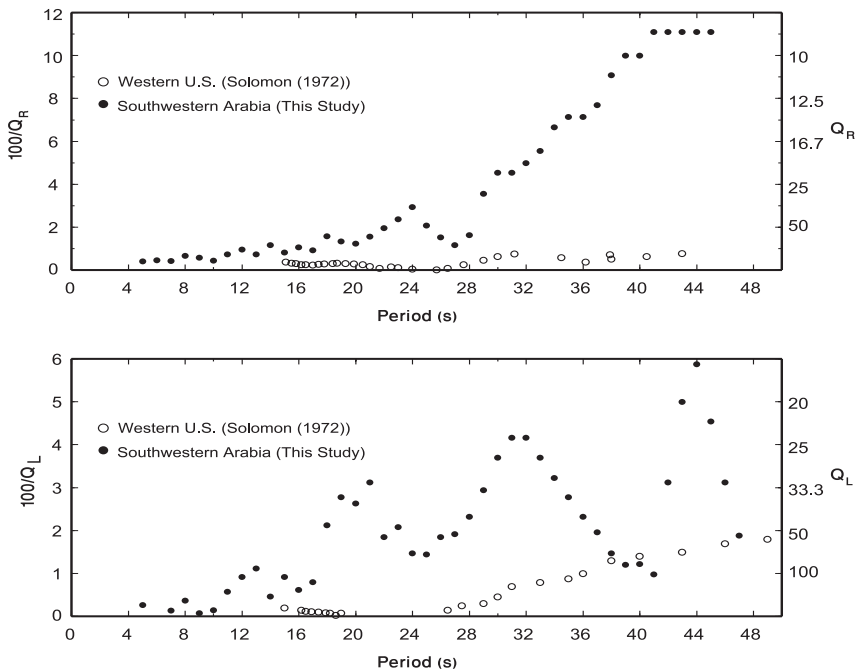


Fig. 6. Comparison of Q_R and Q_L of southwestern Arabia and the southern Red Sea region with those of the western United States.

However, by comparing only the short period values of γ_R and γ_L for the upper crust with those of other regions, it is found that the region attenuation characteristics are similar also to those of tectonically active regions. This is clearly demonstrated in Fig. 7 and 8, which compare the results from this study with data from 12 other different regions of the world. This comparison strongly supports the conclusion that the upper crust of the Arabian shield has high attenuation properties unlike similar stable regions of the world.

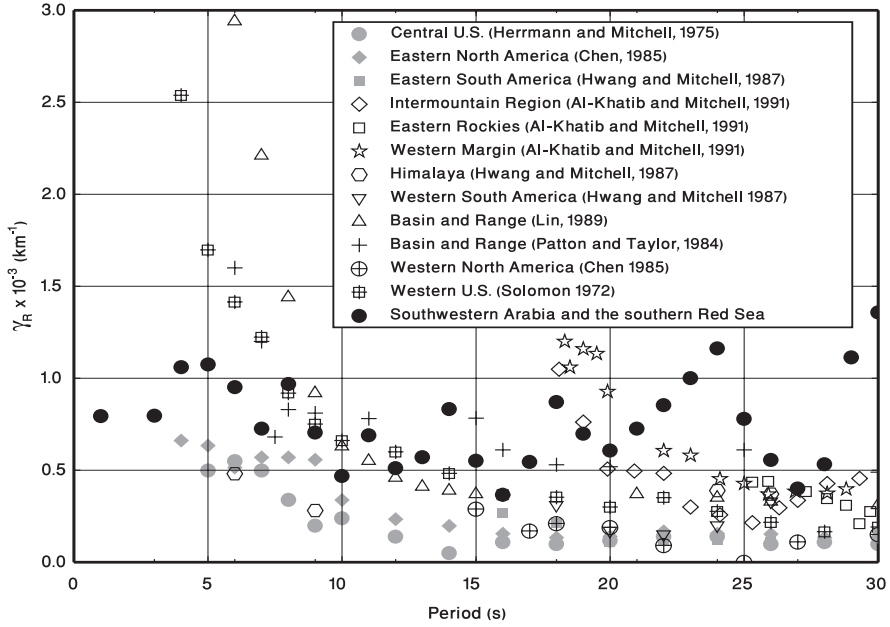


Fig. 7. Comparison between γ_R obtained in this study and γ_R from 12 other Stable and tectonic regions in the world.

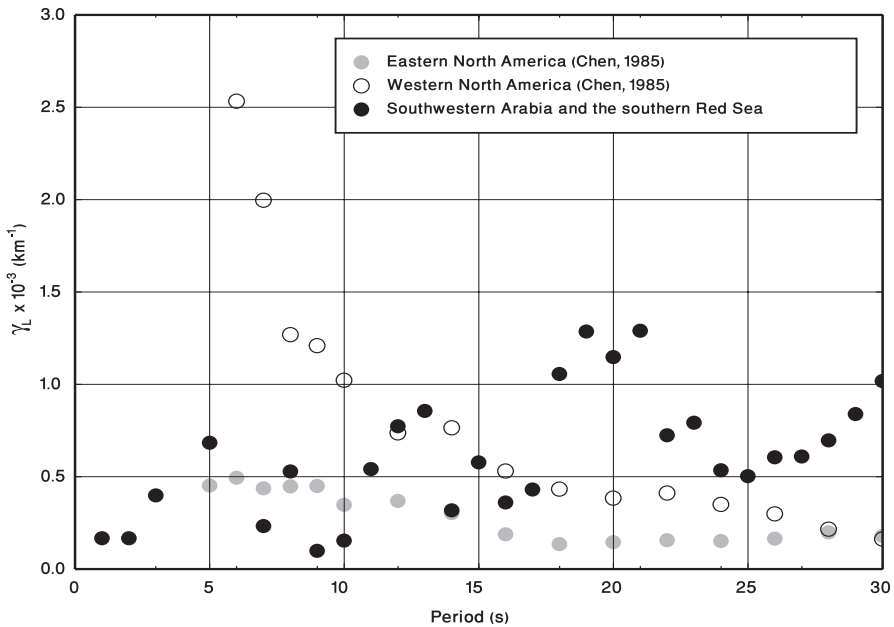


Fig. 8. Comparison between γ_L obtained in this study and γ_L of eastern and western North America.

It should be emphasized, however, that since the path studied spans two tectonic regions, a small part of the southern Red Sea and the southwestern Arabian Peninsula, the measured attenuation is likely some average of the two different areas, and further studies using paths that traverse the Arabian shield only should be made to obtain its attenuation values for the sake of hazard evaluations. The results obtained indicate that the attenuation of seismic waves in this region is high compared to other regions. Surface waves quality factors at short periods are comparable to the values of Q_β for the upper crust obtained by Seber and Mitchell (1992); and Mokhtar (1987). Seismic waves attenuation for Arabia is believed to be much higher than the attenuation in other stable regions such as the eastern United States and the Canadian Shield regions (Seber and Mitchell, 1992). The influence of the ongoing tectonic processes in the Red Sea rift and in neighboring East African rift system clearly has its impact on the degree of seismic waves attenuation in the region.

The process of evolution of the Arabian shield is very important in the interpretation of the present work since it may explain the anelastic attenuation properties of seismic waves in the Arabian plate. If similar processes of evolution were associated with the formation of other parts of the Arabian plate, then partial melting in the upper mantle and the extensive deformations in the crust that may be associated with these tectonic processes could explain very well the high attenuation of seismic surface waves observed in this region. Further investigations are highly recommended using additional seismic data from the national seismic network of Saudi Arabia to map the variations of the elastic and anelastic properties of the Arabian plate.

Acknowledgment

The author would like to express his thanks to the (IRIS/IDA) IRIS GSN/ UNIVERSITY of California, San Diego, and Institute de Physique du Globe de Paris (IPGP) for providing the data of Ar Rayn (Saudi Arabia) and Arta Tunnel, Djibouti through IRIS.

References

- Al-Khatib, H.H. and Mitchell, B.J.** (1991) Upper mantle anelasticity and tectonic evolution of western United States from surface wave attenuation, *J. Geophys. Res.*, **96**: 1829-1846.
- Alshanti, A.M.S.** (1992) *The Geology of the Arabian Shield*, Jeddah: King Abdulaziz Univ. Press, 219 p (*in Arabic*).
- Anderson, D.L., Ben-Menahem, A. and Archambeau, C.B.** (1965) Attenuation of seismic energy in the upper mantle, *J. Geophys. Res.*, **70**: 1441-1448.
- Anderson, D.L. and Sammis, C.** (1970) Partial melting and the low-velocity zone, *Phys. Earth Planet. Interiors*, **3**: 41-50.

- Báth, M.** (1982). *Spectral Analysis in Geophysics*, Development in Solid Earth Geophysics, 7, Amsterdam: Elsevier Scientific Publishing Company, 563.
- Bender, B.** (1984) Incorporating acceleration variability into seismic hazard analysis, *Seism. Soc. Am. Bull.*, **74**: 1451-1467.
- Ben-Menahem, A.** (1965) Observed Attenuation and Q values of seismic surface waves in the upper mantle, *J. Geophys. Res.*, **70**: 4641-4651.
- Chen, J.J.** (1985) Lateral variation of surface wave velocity and Q structure beneath North America, *Ph.D. Thesis*, Saint Louis Univ., St. Louis, Mo., U.S.A., 227 p.
- Dziewonski, A.M. and Anderson, D.L.** (1981) Preliminary reference Earth model, *Phys. Earth Planet. Int.*, **25**: 297-356.
- Ghalib, H.A.A.** (1992) Seismic velocity structure and attenuation of the Arabian plate, *Ph.D. Thesis*, Saint Louis University, Saint Louis, Missouri, U.S.A., 314 p.
- Gettings, M.E., Blank, H.R., Mooney, W.D. and Healy, J.H.** (1986) Crustal structure of the southwestern Saudi Arabia, *J. Geophys. Res.*, **91**: 6491-6512.
- Healy, J.H., Mooney, W.D., Blank, H.R., Gettings, M.E., Kohler, W.M., Lamson, R.J. and Leons, L.E.** (1982) Saudi Arabian seismic deep-refraction profile. Final Project Report., *Saudi Arabian Deputy Ministry of Mineral Resources, Open File Report*, USGS-OF02-37, 429 p.
- Herrmann, R.B. and Mitchell, B.J.** (1975) Statistical analysis and interpretation of surface-wave anelastic attenuation data for the stable interior of North America, *Bull. Seism. Soc. Am.*, **65**: 1115-1128.
- Hwang, H.J. and Mitchell, B.J.** (1987) Shear velocities, Q_{β} , and the frequency dependence of Q_{β} in stable and tectonically active regions from surface wave observations, *Geophys. J.R. Astron. Soc.*, **90**: 575-613.
- Knox, R.P., Nyblade, A.A. and Langston, C.A.** (1998) Upper mantle S velocities beneath Afar and western Saudi Arabia from Rayleigh wave dispersion, *Geophysical Res. Let.*, **25**: 4233-4236.
- Lin, W.J.** (1976) Rayleigh wave attenuation in the Basin and Range provinces, *M.S. Thesis*, Saint Louis Univ., St. Louis, Mo., U.S.A.
- Makris, J. and Ginzburg, A.** (1987) The Afar depression: transition between continental rifting and sea-floor spreading, *Tectonophysics*, **141**: 199-214.
- McGuire, R.K. and Shedlock, K.M.** (1981) Statistical uncertainties in seismic hazard evaluation in the United States, *Seism. Soc. Am. Bull.*, **71**: 1287-1308.
- Menzies, M.A., Baker, J., Bosence, D., Dart, C., Davison, I., Hurford, A., Al'Subbary, M.A. and Yelland, A.** (1992) The timing of magmatism, uplift and crustal extensions; Preliminary observations from Yemen, *Geol. Soc. Spec. Pub.*, Geol. Soc. London, **68**: 293-304.
- Mitchell, B.J.** (1975) Regional Rayleigh wave attenuation in North America, *J. Geophys. Res.*, **80**: 4904-4916.
- Mitchell, B.J., Yacoub, N.K. and Correig, A.C.** (1977) A summary of seismic surface wave attenuations and its regional variations across continents and oceans, in: *The Earth Crust, Am. Geophys. Union Monograph*, **20**: Washington, D. C.
- Mitchell, B.J.** (1980) Frequency dependence of shear wave internal friction in the continental crust of eastern North America, *J. Geophys. Res.*, **85**: 5212-5218.
- Mokhtar, T.A.** (1987) Seismic velocity and Q model for the shallow structure of the Arabian Shield from short period Rayleigh waves, *Ph.D. Thesis*, Saint Louis University, Saint Louis, Missouri, U.S.A., 168 p.
- Mokhtar, T.A.** (1995) Phase velocity of the Arabian platform and its attenuation characteristics by wave-form modeling, *J. King Abdulaziz Univ. Earth Sci.*, **8**: 23-45.

- Mokhtar, T.A.** (2004) Variations of the Crustal Structure of Arabia, *Journal of King Abdulaziz University, Earth Sciences*, **15**: 1-27.
- Mokhtar, T.A., Herrmann, R.B. and Russell, D.R.** (1988) Seismic velocity and Q model for the shallow structure of the Arabian shield from short period Rayleigh waves, *Geophysics*, **53**: 1379-1387.
- Mokhtar, T.A. and Al-Saeed, M.M.** (1994) Shear wave velocity structures of the Arabian Peninsula, *Tectonophysics*, **230**: 105-125.
- Mokhtar, T.A., Ammon, C.J., Herrmann, R.B. and Ghalib, H.A.A.** (2001) Surface wave velocities across Arabia, *Pure and Applied Geophysics*, **158**: 1425-1444.
- Patton, H.J. and Taylor, S.R.** (1984) Q structure of the Basin and Range from surface waves, *J. Geophys. Res.*, **89**: 6929-6940.
- Ritsema, J. and Allen, R.M.** (2003) The elusive mantle plume, *Earth and Planet. Sci. Let.*, **207**: 1-12.
- Ritsema, H.J., van Heijst, J.H. and Woodhouse, J.H.** (1999) Complex shear velocity structure imaged beneath Africa and Iceland, *Science*, **286**: 1925-1928.
- Rodgers, A.J., Walter, W.R., Mellors, R.J., Al-Amri, A.M.S. and Zhang, Y.S.** (1999) Lithospheric structure of the Arabian shield and platform from complete regional waveform modelling and surface wave group velocities, *Geophys. J. Int.*, **138**: 871-878.
- Sandvol, E., Al-Damegh, K.A., Calvert, A., Seber, D., Barazangi, M., Mohamad, R., Gök, Turkelli, R.N. and Gürbuüz, C.** (2001) Tomographic imaging of Lg and Sn propagation in the Middle East, *Pure and Applied Geophysics*, **158**: 1121-1163.
- Schmidt, D.L., Hadley, D.G. and Stoesser, D.B.** (1979) Late Proterozoic crustal history of the Arabian shield, southern Najd province, Kingdom of Saudi Arabia, evolution and mineralization of the Arabian-Nubian shield, *I.A.G. Bull.*, **3** (2): 41-58.
- Seber, D.** (1990) Attenuation of surface waves across the Arabian peninsula, *M.Sc. Thesis*, Saint Louis University, Saint Louis, Missouri, U.S.A., 106 p.
- Seber, D. and Mitchell, B.** (1992) Attenuation of surface waves across the Arabian peninsula, *Tectonophysics*, **204**: 137-150.
- Solomon, S.C.** (1972) Seismic-wave attenuation and partial melting in the upper mantle of North America, *J. Geophys. Res.*, **77**: 1483-1502.
- Thenhaus, P.C., Algermissen, S.T., Perkins, D.M., Hanson, S.L. and Diment, W.H.** (1989) Probabilistic estimates of the seismic ground-motion hazard in western Saudi Arabia, *U.S. Geological Survey Bulletin 1868*, prepared in cooperation with the Ministry of Petroleum and Mineral Resources, Deputy Ministry of Mineral Resources, Kingdom of Saudi Arabia, 40 p.
- Toksöz, M.N., Johnson, D.H. and Timur, A.** (1979) Attenuation of seismic waves in dry and saturated rocks, *Geophysics*, **44**: 681-690.
- Walsh, J.B.** (1966) Seismic wave attenuation in rock due to friction, *J. Geophys. Res.*, **71**: 2591-2599.
- Winkler, K.W. and Nur, A.** (1982) Seismic attenuation: Effects of pore fluids and frictional sliding, *Geophysics*, **47**: 1-15.

الاضمحلال غير المرن للموجات السطحية تحت منطقة جنوب غرب شبه الجزيرة العربية وجنوب البحر الأحمر

طلال علي مختار

قسم الجيوفيزياء، كلية علوم الأرض، جامعة الملك عبد العزيز
ص.ب. ٨٠٢٠٦، جدة ٢١٥٨٩، المملكة العربية السعودية

المستخلص. تمت دراسة معاملات الاضمحلال للموجات السيزمية السطحية في منطقة جنوب غرب شبه الجزيرة العربية وجنوب البحر الأحمر باستخدام طريقة نسبة المحطة. واستخدم في ذلك بيانات موجات رايلي وموجات لف المسجلة في محطتين من محطات الشبكة العالمية GSN هما محطة RAYN ومحطة ATD، وذلك لحساب معاملات اضمحلال رايلي ولف وكذلك Q_L و Q_R في المنطقة بين المحطتين. محطة RAYN تقع في وسط شبه الجزيرة العربية بينما تقع ATD على الشاطئ الغربي لجنوب البحر الأحمر على منخفض عفار. ووجد أن معامل الاضمحلال لموجات رايلي γ_R يتغير من أدنى قيمة له تبلغ 0.3×10^{-4} كم^{-١} عند زمن دوري ٢٧ ثانية وأعلى قيمة بمقدار $9 \times 22 \times 10^{-4}$ كم^{-١} عند زمن دوري ٤٤ ثانية. كما تم حساب γ_L ووجد أنها تتذبذب بين قيمة دنيا تبلغ $28 \times 2 \times 10^{-4}$ كم^{-١} عند ٦ ثواني وقيمة عظمى تبلغ $10, 81 \times 10^{-4}$ كم^{-١} عند ٢٣ ثانية. ووجد أن متوسط قيمة Q_R للقشرة العليا 100 ومتوسط قيمة Q_L للقشرة العليا 160 . إن اضمحلال الموجات السطحية تحت القشرة عالي جداً في هذه المنطقة. ويمكن تفسير ذلك من خلال النشاط التكتوني الجاري في منطقة البحر الأحمر ومنخفض عفار. إن درجات الحرارة العالية والانصهار الجزئي لمكونات ما تحت القشرة يمكن أن ينتج عنه درجات عالية من الامتصاص عند الأزمنة الدورية الطويلة. أما عند تلك الأزمنة الدورية القصيرة (أقل من ٢٧ ثانية)، فإن درجة الاضمحلال تكون أقل، ولكنها لا تزال أكبر منها في المناطق الثابتة من العالم. إن نتائج البحث تؤكد على الشواهد السابقة بأن الصفيحة العربية، خلافاً للمناطق الثابتة، يتميز بدرجة عالية من الاضمحلال للموجات الزلزالية في القشرة وفي الوشاح العلوي يمكن مقارنتها بمناطق عدة ذات نشاط تكتوني في العالم.